SEMARAK ILMU PUBLISHING
202103268166(003316878-P)

Journal of Advanced Research in Applied Sciences and Engineering Technology

Journal homepage:
https://semarakilmu.com.my/journals/index.php/applied_sciences_eng_tech/index
ISSN: 2462-1943


# Performance Evaluation of Edge-Based Segmentation Methods for Electrical Tree Image Analysis in High-Voltage Experiments

Mohd Annuar Mohd Isa[1,*], Mohamad Firdaus Azahari[1], Mohamad Nur Khairul Hafizi Rohani[1], Baharuddin Ismail[1], Afifah Shuhada Rosmi[1], Mohamad Kamarol Jamil[2], Noor Syazwani Mansor[3], Abdullahi A. Mas'ud[4], Firdaus Muhammad-Sukki[5]

[1] Faculty of Electrical Engineering &Technology, Universiti Malaysia Perlis (UniMAP), 02600 Arau, Perlis, Malaysia
[2] School of Electrical and Electronic Engineering, Universiti Sains Malaysia, 11700 Gelugor, Pulau Pinang, Malaysia
[3] Faculty of Electrical Engineering, Universiti Teknologi Malaysia, 81310 Johor Bahru, Johor, Malaysia
[4] Department of Electrical Engineering, Jubail Industrial College, Al Jubail 35718, Saudi Arabia
[5] School of Computing, Engineering & the Built Environment, Edinburgh Napier University, Merchiston Campus, 10 Colinton Road, Edinburgh EH10 5DT, United Kingdom

**ARTICLE INFO**

***Article history:***
Received 10 December 2023
Received in revised form 7 May 2024
Accepted 6 June 2024
Available online 10 July 2024

***Keywords:***
Partial discharge; electrical tree; XLPE; Image processing; edge segmentation

**ABSTRACT**

This research evaluates the performance of edge-based segmentation methods in analysing two-dimensional (2D) electrical tree images obtained during high-voltage (HV) electrical tree experiments. Non-uniform illumination in 2D optical images poses challenges in accurately extracting and measuring the original treeing image. Edge segmentation emerges as a promising solution to precisely distinguish tree structures from the insulation background within the image. Cross-linked polyethylene (XLPE) samples were subjected to HV stress for real-time propagation observation, followed by extraction and segmentation of treeing images using edge-based operators. The findings emphasize the superiority of the Roberts edge operator in accurately detecting electrical trees, showcasing the highest average accuracy of 97.01% and 99.58% specificity, while also demonstrating relatively high sensitivity. Moreover, the Roberts method provide much precisely measures the propagation length and width than conventional measurement method, closely approximating the actual tree measurements. This research emphasizes the significance of accurate segmentation for investigating electrical tree propagation in XLPE materials and provides recommendations for future research, especially in HV XLPE cable manufacturing.

## 1. Introduction

XLPE has been extensively utilized and is outperforming other types of medium-to-high-voltage (HV) cables due to its outstanding electrical qualities, lightweight construction, and high transmission limit [1,2]. Although XLPE cable has good thermal stability and can sustain high temperatures, it is susceptible to partial discharge (PD), which may cause power failure and breakdown [3,4]. The majority of the time, PD is generated by the manufacturing process or by power cable accessories

* *Corresponding author.*
*E-mail address: annuar@unimap.edu.my*

https://doi.org/10.37934/araset.48.1.213226

such as joints or terminations [5,6]. Internal discharge in cable insulation is most often caused by electrical tree initiation in cable insulation.

Impurities and protrusions, especially metal ones, are the most dangerous things that can cause XLPE cables to short out or lose their insulation [7]. Needle-plane geometries were used in a laboratory setting to simulate the effect of impurities and protrusions on local fields and electrical trees [8,9], where powerful fields may be generated with little input voltage, and where tree development in see-through XLPE materials can be readily monitored. To better understand electrical tree development, especially in XLPE insulating material, it is now common practice to conduct direct optical inspections of the polymer under HV stress [10,11]. Image processing methods, such as segmentation, can be employed to these microscope images for a more precise measurement of the tree's expansion. When analysing details in an optical image, however, the issue of non-uniform illumination and noise remains a significant obstacle that degrades the original image [12-14]. Extensive image segmentation research has helped to produce a variety of segmentation algorithms for several applications in a wide range of disciplines precisely for this reason. Following the trends, this paper presents performance evaluation of electrical tree segmentation using edge-based method of two-dimensional (2D) images obtained from HV treeing experiment on XLPE insulation material.

### *1.1 Literature Review*

Dissado's treeing growth model categorizes electrical tree phenomenon into a three-stage process, starting with inception, followed by propagation, and culminating in the runaway and breakdown stage [15]. Electrical trees initiate when they emerge from regions with contaminants or voids, leading to an electric field surpassing the dielectric strength of XLPE insulation. This shift in the dielectric constant results in an increased electrical field, causing gas ionization within the void and the formation of PD. Subsequently, the electrical tree continues to grow and propagate in the form of a branch, bush, or a combination of both towards the opposite electrode. Branch-type trees have fine filamentary channels stemming from limited branches, while bush-type trees are densely packed with overlapping branches forming a solid bush-shaped mass. During propagation, the electric field at the tree's tip intensifies. Eventually, the growth speed accelerates, leading to a runaway effect just before the insulation material experiences irreversible breakdown.

Over time, various quantitative measurement parameters have been employed to assess electrical trees. Two important parameters are tree length (L), which measures the Euclidean distance from the tree's initiation point to the farthest tree tip in the 2D projected treeing image along the direction of the electric field, and tree width (D), representing the extent of the tree channels' spread in the 2D projected image perpendicular to the electric field direction [16-18], as illustrated in Figure 1.

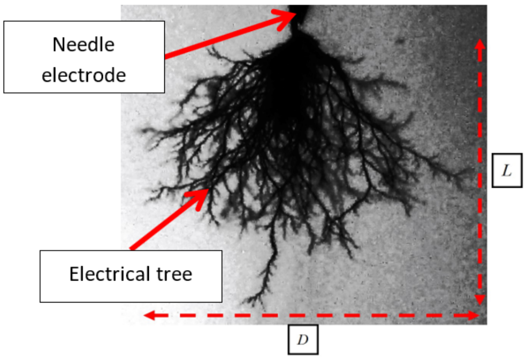


**Fig. 1.** Tree growth measurement parameters of length (L) and width (D)

### *1.2 Edge Segmentation Methods*

Measuring the propagation length and width of an electrical tree from an image requires expertise in image processing and measurement techniques. Although image editing software allows direct measurements, researchers often encounter challenges related to illumination variance and noise in 2D optical images [19]. To perform accurate edge segmentation, various edge operators are commonly employed, which detect and emphasize boundaries between different regions in an image. Several widely used edge operators are available for edge segmentation, including the Prewitt, Sobel, Roberts, Laplacian of Gaussian (LoG) and Canny detectors. Table 1 provides a summary of edge operators categorized by their respective methods of operation.

**Table 1**
Method of operations for edge operators

| Edge Operator | Method of operations | Common Mask Used |
|---|---|---|
| Prewitt | Prewitt operator involves convolving the image with two 3x3 mask to detect edges in the horizontal and vertical directions, $G_x$ and $G_y$ | $\begin{bmatrix} -1 & 0 & 1 \\ -1 & 0 & 1 \\ -1 & 0 & 1 \end{bmatrix}$ $G_x$ $\begin{bmatrix} -1 & -1 & -1 \\ 0 & 0 & 0 \\ 1 & 1 & 1 \end{bmatrix}$ $G_y$ |
| Sobel | Sobel operator uses two 3x3 convolution mask for detecting edges in the horizontal and vertical directions, $G_x$ and $G_y$ | $\begin{bmatrix} -1 & 0 & +1 \\ -2 & 0 & +2 \\ -1 & 0 & +1 \end{bmatrix}$ $G_x$ $\begin{bmatrix} +1 & +2 & +1 \\ 0 & 0 & 0 \\ -1 & -2 & -1 \end{bmatrix}$ $G_y$ |
| Roberts | The Roberts operator uses two 2x2 convolution mask for detecting edges in diagonal directions, $G_x$ and $G_y$ | $\begin{bmatrix} +1 & 0 \\ 0 & -1 \end{bmatrix}$ $G_x$ $\begin{bmatrix} 0 & +1 \\ -1 & 0 \end{bmatrix}$ $G_y$ |
| LoG | It combines Gaussian smoothing with Laplacian operators. The Gaussian filter is applied to smooth the image and the convolution mask size lowers the sensitivity to noise. Given a pixel $(x, y)$, with standard deviation, $\sigma$, LoG can be expressed as: $LoG = -\frac{1}{\pi\sigma^4}\left[1 - \frac{x^2+y^2}{2\sigma^2}\right]e^{\frac{x^2+y^2}{2\sigma^2}}$ | $\begin{bmatrix} 0 & 0 & -1 & 0 & 0 \\ 0 & -1 & -2 & -1 & 0 \\ -1 & -2 & 16 & -2 & -1 \\ 0 & -1 & -2 & -1 & 0 \\ 0 & 0 & -1 & 0 & 0 \end{bmatrix}$ 5x5 convolution mask |

| | | |
|---|---|---|
| Canny | Multi-stage approach known for precise edge localization and noise reduction. It involves several steps including Gaussian smoothing, gradient calculation, non-maximum suppression, and edge tracking by hysteresis [20]. | $\frac{1}{159}\begin{bmatrix} 2 & 4 & 5 & 4 & 2 \\ 4 & 9 & 12 & 9 & 4 \\ 5 & 12 & 15 & 12 & 5 \\ 4 & 9 & 12 & 9 & 4 \\ 2 & 4 & 5 & 4 & 2 \end{bmatrix}$ 5x5 Gaussian smoothing mask |

The effectiveness of edge operators for image segmentation relies on their unique strengths and weaknesses, highlighting the significance of selecting the most suitable method based on specific image characteristics and application requirements. The objective of this research is to comprehensively evaluate the edge-based segmentation methods mentioned above. These methods are employed for the extraction of electrical tree structures from original 2D images obtained during HV experiments. By conducting a rigorous analysis and comparison, this study aims to determine the most precise and efficient approach for this critical task.

## 2. Methodology

### *2.1 XLPE Sample Preparation*

The insulation sample utilized in this experiment is composed of XLPE materials and Ogura® needles arranged in a planar-to-plane configuration. Firstly, the XLPE beads as shown in Figure 2(a), were subjected to compression moulding in specially designed iron mould and then sliced into rectangular shaped with dimension 15 mm × 25mm × 2mm. The sample is heated in the oven at 120˚C for 10 minutes before needle insertion process. The needle electrode of 1 mm diameter with tip angle 30˚ was inserted slowly into sample with the gap between the needle tip and plane electrode is 2 mm as shown in Figure 2(b) and later rested in the oven for further 10 minutes at 60˚C to remove any mechanical stress.

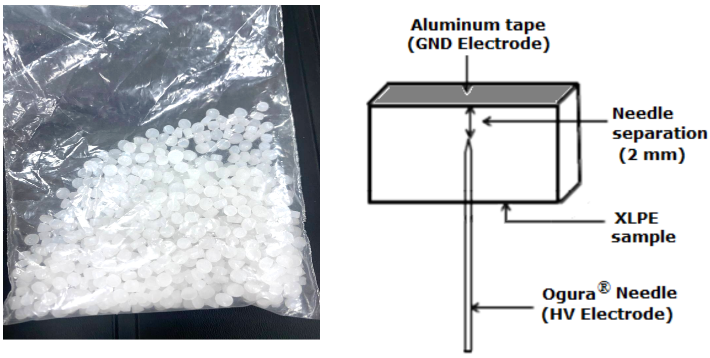


(a) (b)

**Fig. 2.** Sample preparation (a) XLPE beads (b) Planar-to-plane electrode configuration

### *2.2 Experimental Setup for Treeing Acquisition*

The experimental work was conducted at the School of Electrical and Electronic, University of Science Malaysia, Engineering Campus, Malaysia. The experimental setup comprised a 50 Hz 230/140 kV high voltage transformer, a 2.5 MΩ limiting resistor and a 1000:1 capacitive divider as in Figure 3. The insulation sample was placed in a rectangular container filled with mineral oil and placed under a microscope. The needle electrode was connected to the high voltage source, while the opposite electrode was connected to the ground. The purpose of the mineral oil was to prevent electrical flashover during the experiment. The applied voltage was ramped up at a rate of 1 kV/sec to determine the electrical tree inception voltage (TIV). Propagation of the electrical tree was observed and recorded using a charge-coupled device (CCD) camera. The propagation of the electrical tree, which initiated upon the application of voltage, was analysed for a maximum duration of 60 minutes ($t_0$ to $t_{60}$) for all five samples.

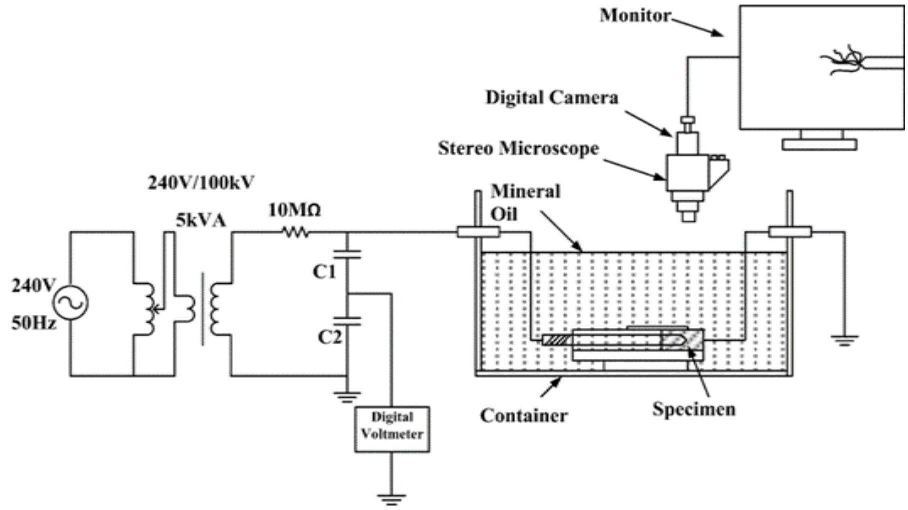


**Fig. 3.** Electrical tree data acquisition setup

### *2.3 Image Pre-Processing, Segmentation and Analysis*

During the pre-processing stage, electrical tree images from each sample were initially extracted from the original recording, taking into account their respective treeing durations. Later, these extracted images were transformed into greyscale representations. Greyscale conversion simplifies subsequent segmentation steps by focusing solely on variations in pixel intensity, effectively eliminating the complexity of colour information. Following the grayscale conversion, five distinct edge-based segmentation methods including Prewitt, Canny, Sobel, Roberts, and LoG were employed to classify the pixels corresponding to tree structures from those representing the background.

In the final stage, the output of image segmentation for each technique will be assessed using widely employed performance metrics such as accuracy, sensitivity and specificity. Table 2 represents the mathematical expression for each metric where True Positive (TP) refers to the count of pixels or instances correctly identified as foreground, whereas True Negative (TN) denotes background pixels that were correctly identified as such. False Positive (FP) indicates the number of background pixels that were mistakenly classified as foreground, and False Negative (FN) represents foreground pixels that were incorrectly classified as background pixels.

**Table 2**
Evaluation metrics

| Assessment | Formula |
|---|---|
| Accuracy | $\frac{TP+TN}{TP+TN+FP+FN}$ |
| Sensitivity | $\frac{TP}{TP+FN}$ |
| Specificity | $\frac{TN}{FP+TN}$ |

Accuracy quantifies the proportion of correct classifications. Sensitivity, also known as recall, measures the correct identification of foreground pixels in relation to the total number of foreground pixels. Specificity rate, on the other hand, indicates the ratio of correctly classified background pixels to the total number of background pixels. This quantitative analysis aims to compare the technique's segmentation performance to a pre-generated reference image of the tree. The reference image, also known as ground truth (GT) image is obtained through precise hand-labelling techniques with the assistance of open-source image editing software based on the original treeing image. For instance, original and the respective reference images for the five image samples are depicted in Table 3.

**Table 3**
Comparison between original treeing images and the respective ground truth

| | Sample Number | | | | |
|---|---|---|---|---|---|
| | $S_1$ | $S_2$ | $S_3$ | $S_4$ | $S_5$ |
| Original | | | | | |
| Ground truth | | | | | |

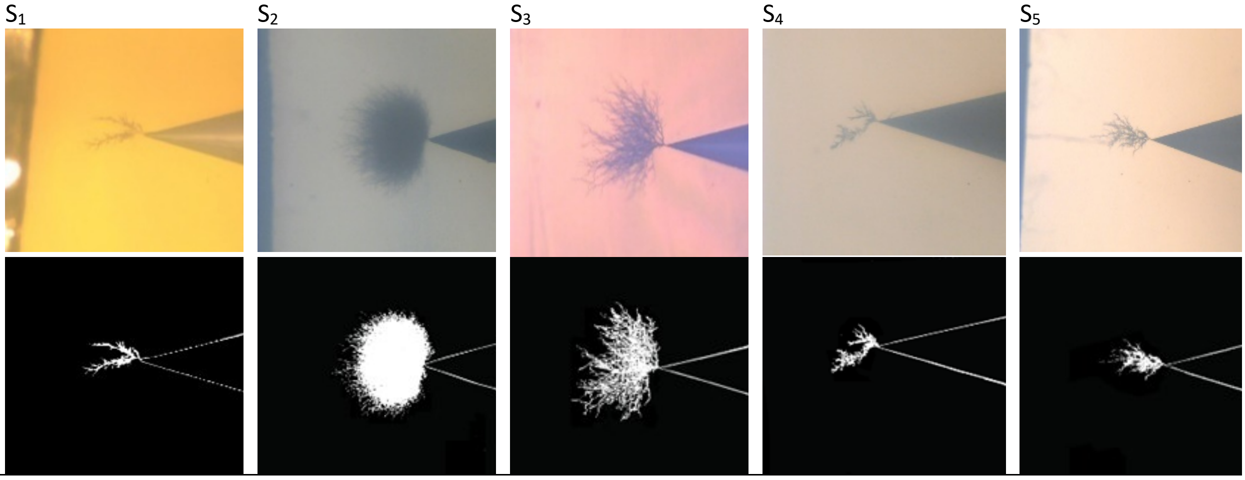

The image samples, labelled from $S_1$ to $S_5$ exhibit distinct illumination conditions and varying electrical tree shapes. Specifically, $S_1$ and $S_4$ feature branch-type trees, whereas $S_2$ displays a bush-type tree. The mixed-type structures are represented by $S_3$ and $S_5$. Figure 4 represents the complete process flow for evaluating the performance of edge segmentation methods in electrical tree image analysis.

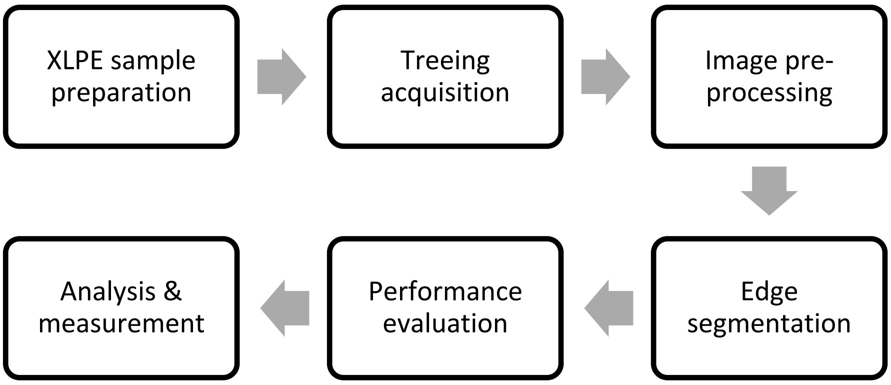


**Fig. 4.** Process flow of performance evaluation of edge segmentation methods for electrical tree image analysis

## 3. Results

The complete electrical tree segmentation procedure was conducted using Microsoft Windows 10, Intel® Core™ i5, CPU 2.5 GHz with 8 GB RAM, and MATLAB R2017a. The GT image serves as the basis for evaluating the performance of all segmentation approaches, using performance metric such as accuracy, sensitivity, and specificity. The image segmentation output based on all approaches used is summarised in Table 4 for all samples at $t_{60}$. Based on visual observation, it is evident that Canny and LoG methods exhibit the least satisfactory performance in terms of image segmentation among all the methods. These methods exhibit a higher misclassification of background pixels as foreground pixels compared to other edge operators. This increased false-alarm categorization is likely attributed to Canny's and LoG's sensitivity to noise, including non-uniform lighting variations present in the original treeing images. On the other hand, Prewitt, Roberts, and the Sobel filter demonstrate improved segmentation results with only a small portion of background misclassified as foreground in each image segmentation output.

**Table 4**
Treeing segmentation performance comparison

| Technique | Sample | | | | |
|---|---|---|---|---|---|
| | $S_1$ | $S_2$ | $S_3$ | $S_4$ | $S_5$ |
| Canny | 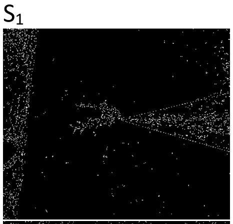 | 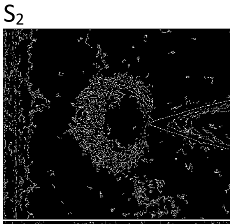 | 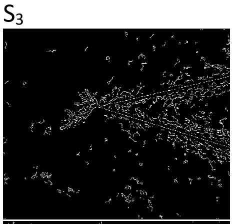 | 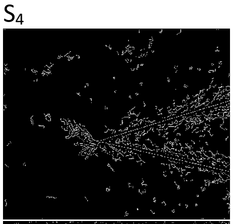 | 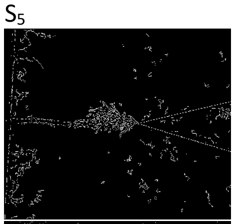 |
| LoG | 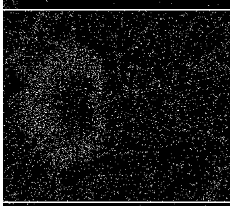 | 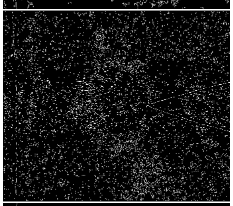 | 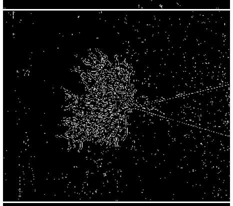 | 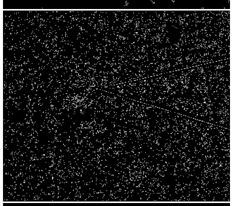 | 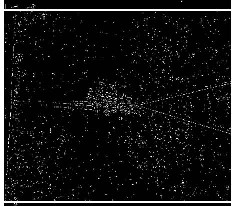 |
| Prewitt | 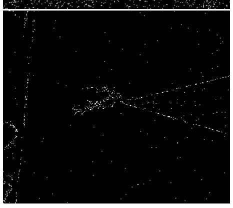 | 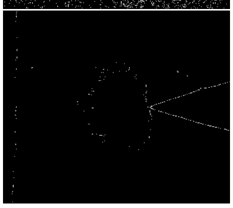 | 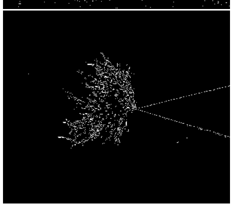 | 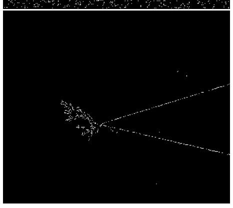 | 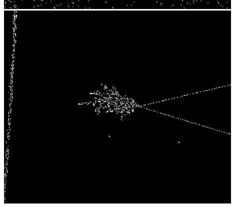 |

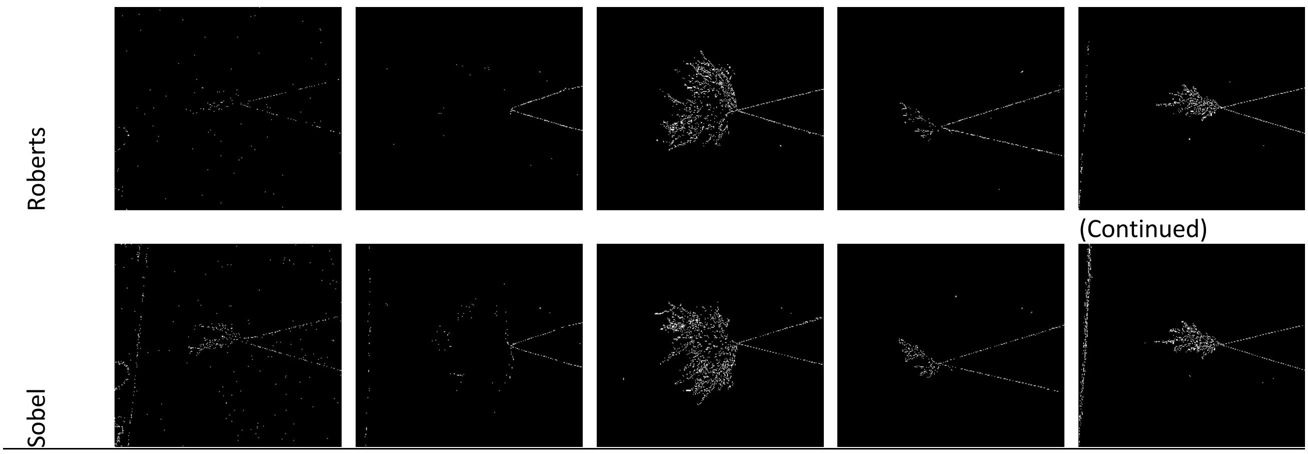


In Figure 5, a comparative analysis is shown, evaluating the performance of different edge-based methods for treeing image segmentation, specifically for branch-type trees in sample $S_1$. Accuracy, sensitivity, and specificity serve as evaluation metrics. Accuracy signifies the overall percentage of correctly identified foreground or electrical tree pixels and their respective background. Sensitivity indicates the proportion of actual tree pixels correctly identified, while specificity measures the proportion of non-tree pixels correctly identified as background. Among the methods tested, Roberts achieves the highest accuracy of 98.76% and 99.90% specificity but records low sensitivity rate. On the other hand, Canny exhibits the highest sensitivity rate of 9.90% but slightly lower accuracy and specificity compared to others. The weakest performance in treeing image segmentation for $S_1$ is observed with the LoG method, which exhibits the lowest scores in accuracy and specificity and relatively low sensitivity.

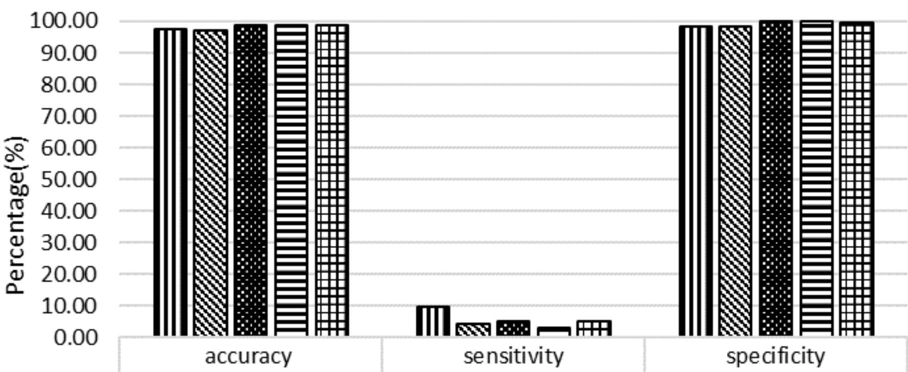


| | accuracy | sensitivity | specificity |
|---|---|---|---|
| Canny | 97.29 | 9.90 | 98.33 |
| Log | 97.09 | 4.49 | 98.20 |
| Prewiit | 98.65 | 5.02 | 99.77 |
| Roberts | 98.76 | 2.89 | 99.90 |
| Sobel | 98.63 | 5.07 | 99.75 |

**Fig. 5.** Performance comparison of segmentation methods for $S_1$

In the case of bush-type tree in $S_2$,

Fig. **6** illustrates the segmentation evaluation. Prewitt, Roberts, and Sobel demonstrated the most favourable performance in terms of accuracy and specificity, with Prewitt having a slight edge, achieving percentages of 93.06% and 99.67%, respectively. Conversely, the LoG method achieved the lowest scores in accuracy and specificity. As for sensitivity performance, Canny outperformed the other methods with a rate of 11.72% while having relatively low performance with accuracy and specificity.

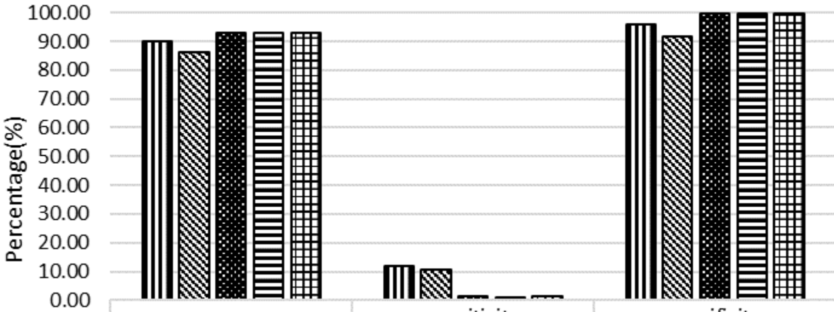


| | accuracy | sensitivity | specificity |
|---|---|---|---|
| Canny | 90.08 | 11.72 | 95.73 |
| Log | 86.42 | 10.64 | 91.88 |
| Prewiit | 93.06 | 1.32 | 99.67 |
| Roberts | 93.02 | 1.13 | 99.64 |
| Sobel | 93.06 | 1.39 | 99.66 |

**Fig. 6.** Performance comparison of segmentation methods for $S_2$

Fig. **7** presents segmentation performance for all methods applied on treeing sample $S_3$. This mixed-type treeing image exhibited relatively low percentage scores, though there was a slight improvement in sensitivity compared to the previous sample, with Canny achieving the highest score of 21.11%. However, both Canny and the LoG method still underperformed in terms of accuracy and specificity, with the LoG method having the poorest overall performance. On the other hand, Prewitt, Sobel, and Roberts consistently maintained high scores in accuracy and specificity.

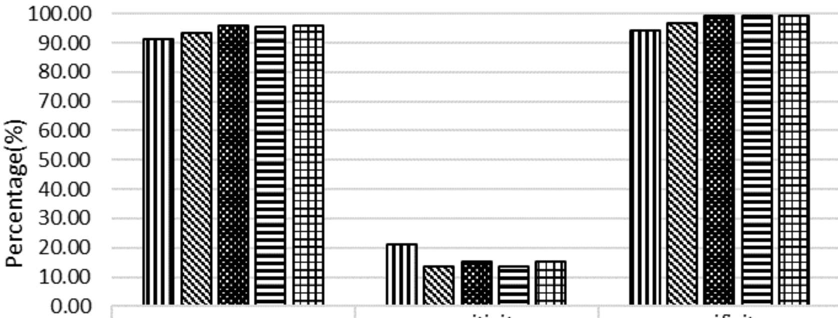


| | accuracy | sensitivity | specificity |
|---|---|---|---|
| Canny | 91.24 | 21.11 | 94.32 |
| Log | 93.25 | 13.60 | 96.75 |
| Prewiit | 95.68 | 15.26 | 99.21 |
| Roberts | 95.65 | 13.70 | 99.25 |
| Sobel | 95.68 | 15.26 | 99.21 |

**Fig. 7.** Performance comparison of segmentation methods for $S_3$

Meanwhile for $S_4$ which represents another branch-type tree structure, similar conclusions can be drawn. Prewitt, Roberts, and Sobel performed exceptionally well in terms of accuracy and specificity scores, while Canny and Sobel exhibited the weakest performance as depicted in

Fig. **8**. Prewitt emerged as the most reliable method, boasting the highest scores of 98.84% and 99.71% for accuracy and specificity, respectively, and demonstrating relatively high sensitivity.

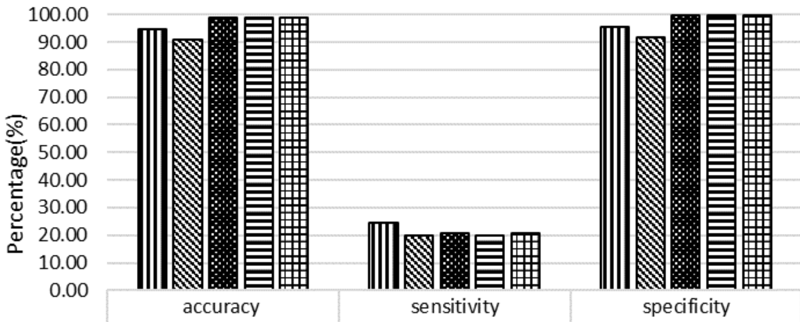


| | accuracy | sensitivity | specificity |
|---|---|---|---|
| Canny | 94.69 | 24.42 | 95.48 |
| Log | 90.71 | 19.97 | 91.50 |
| Prewiit | 98.84 | 20.57 | 99.71 |
| Roberts | 98.81 | 19.97 | 99.68 |
| Sobel | 98.84 | 20.56 | 99.71 |

**Fig. 8.** Performance comparison of segmentation methods for $S_4$

Finally, the segmentation performance of another mixed-type tree in $S_5$ is documented in

Fig. **9**. Among the three usual top performers in previous samples, Roberts proves to be the best suited for segmenting this treeing image, achieving the highest performance across all metrics with 98.82% accuracy, 30.23% sensitivity, and 99.44% specificity. Conversely, LoG and Canny remain the weakest edge operators in segmenting treeing images.

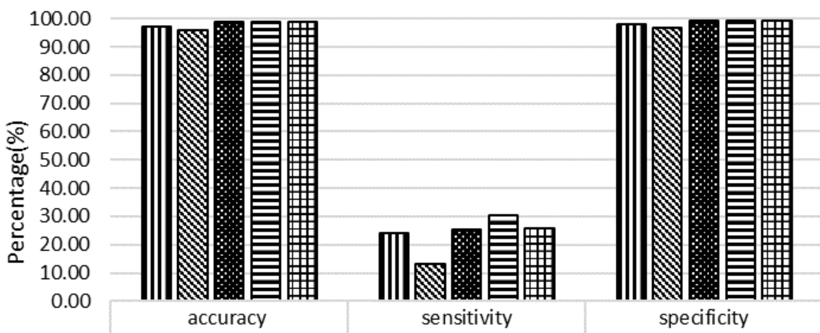


| | accuracy | sensitivity | specificity |
|---|---|---|---|
| Canny | 97.31 | 24.07 | 97.97 |
| Log | 95.94 | 13.07 | 96.69 |
| Prewiit | 98.66 | 25.41 | 99.33 |
| Roberts | 98.82 | 30.23 | 99.44 |
| Sobel | 98.67 | 25.62 | 99.33 |

**Fig. 9.** Performance comparison of segmentation methods for $S_5$

In summary, based on the evaluation of various edge-based segmentation methods on different treeing samples, Roberts consistently emerges as the best segmentation method. It achieved the highest accuracy and specificity average score of 97.01% and 99.58% across all five samples as shown in Figure 10. Although Roberts has a slightly lower average sensitivity rate compared to Canny's 18.24%, the overall performance of Roberts surpasses this limitation, demonstrating its reliability in accurately detecting electrical tree structures. This exceptional performance can be attributed to the Roberts operator's distinctive sensitivity to diagonal edges, which ensures that even the subtlest features within tree images are accurately captured during the segmentation process. The utilization of a diagonal convolution mask in the Roberts method proved particularly effective in detecting tree edges across a range of tree shapes and structures.

On the other hand, the LoG and Canny methods showed weaker performance across different treeing samples. They struggled with accuracy and specificity and were particularly sensitive to noise since both methods are designed to detect edges by identifying rapid changes in pixel intensity. As a result, even slight variations in pixel values due to noise may be incorrectly identified as edges, particularly when non-uniform illumination is present within treeing images. It should be noted that the sensitivity rate is relatively low for all methods across all treeing samples. This is primarily due to the challenges faced by edge operators in detecting dense tree structures caused by overlapping tree branches, particularly in bush-shaped trees. The dense areas exhibit very few edge profiles that can be effectively detected by the edge-based operators, leading to the observed low sensitivity rate in all samples.

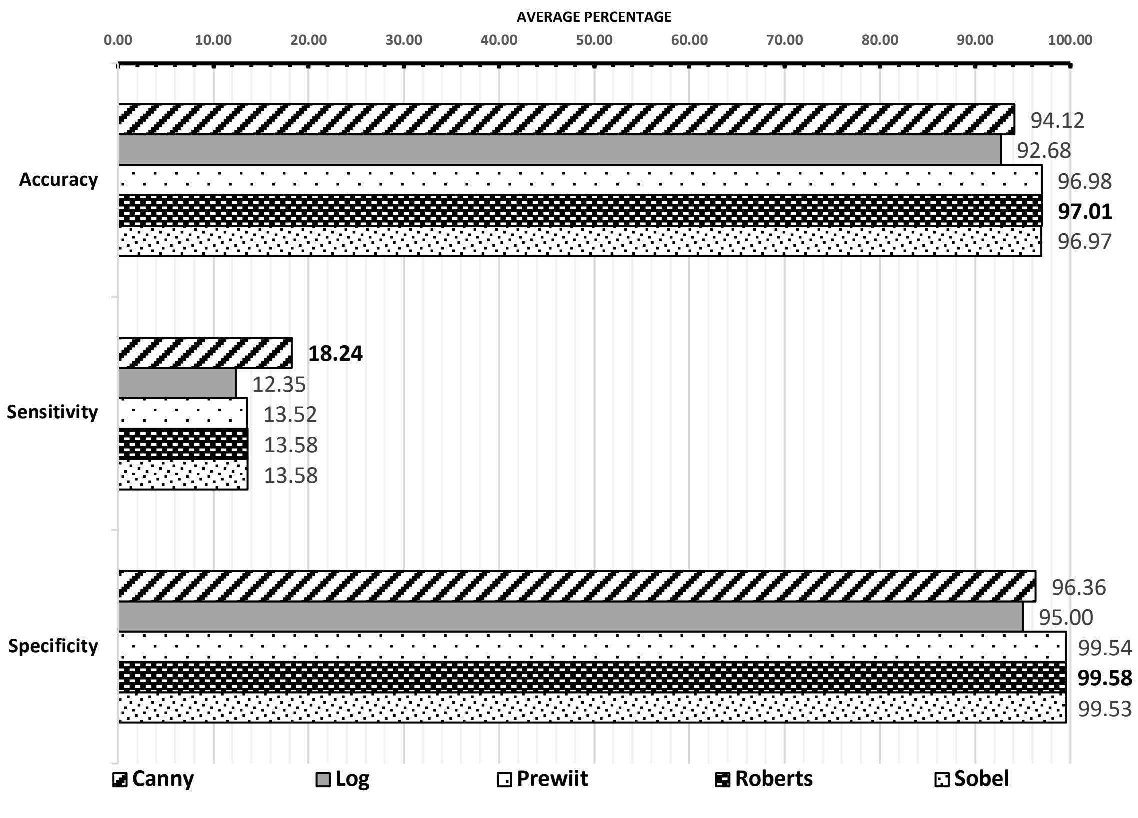


**Fig. 10.** Average performance comparison of segmentation methods across all samples

For a more comprehensive examination of Roberts' segmentation performance on treeing images, we assessed the segmentation results for tree propagation length and width for selected sample $S_3$ for the duration of $t_0 – t_{30}$ of the HV experiment. These measurements were then compared with conventional measurements taken directly from the original image without segmentation, as well as the GT, representing the most accurate representation of the tree propagation structures. Roberts' method displayed minimal deviation error of ±0.15 mm from the GT measurements in terms of tree length and width as depicted in Figure 11(a) and Figure 11(b) respectively, whereas conventional measurements deviated further, particularly in tree width measurement. In conclusion, Roberts' method exhibited a superior level of accuracy, closely resembling the actual presence of the tree structure in the sample.

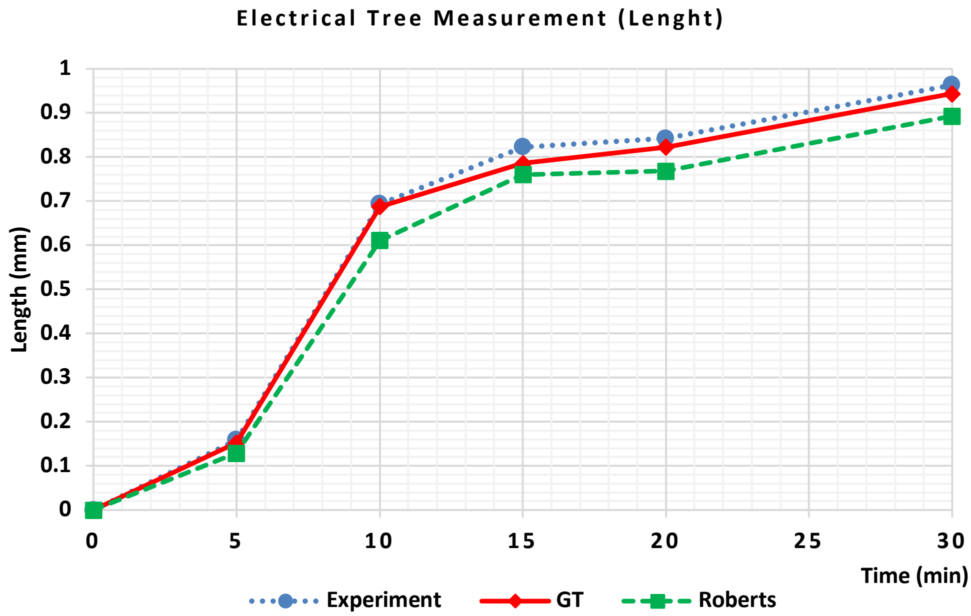


(a)

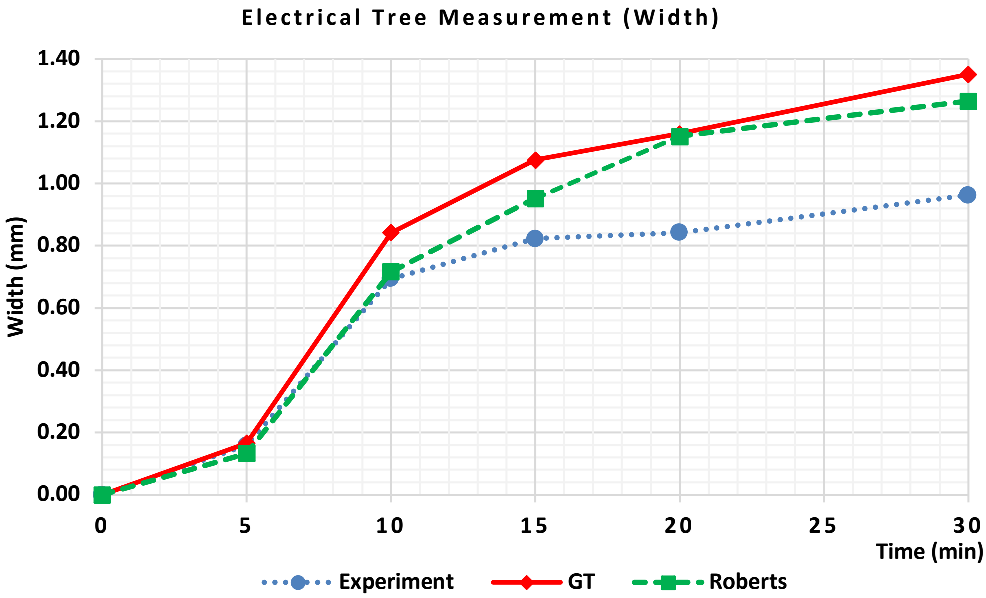


(b)

**Fig. 11.** Tree propagation measurement comparison for selected sample $S_3$ (a) Length (b) Width

## 4. Conclusions

This paper presents a comparative study that assesses the effectiveness of various segmentation methods in classifying the electrical tree structure in 2D treeing images acquired from HV experiment on five different XLPE samples. Different edge-based methods, including Prewitt, Canny, Sobel, Roberts, and LoG, were employed, and their results were analysed using performance metrics such as accuracy, sensitivity, and specificity. Among the evaluated segmentation methods, Roberts operator consistently exhibited the highest reliability in segmenting tree images. It outperformed other methods, achieving an impressive average accuracy of 97.01% and a remarkable average specificity of 99.58%. Furthermore, it demonstrated a relatively higher average sensitivity when compared to the alternative methods, as evidenced by its performance across all five samples. The evaluation of Roberts' segmentation performance on treeing images showcased its ability to accurately measure the tree propagation length and width with acceptable deviations from the ground truth measurements. The outstanding performance can be credited to the Roberts operator's ability to detect diagonal edges effectively, ensuring that even the slightest details in tree images are precisely recognized during the segmentation process. The Roberts operator's use of a diagonal convolution mask proved to be particularly suited for the accurate detection of tree edges in a variety of tree shapes. This attribute significantly contributed to enhancing the effectiveness of the segmentation process. These findings underscore the potential of edge-based segmentation methods, particularly Roberts' method, for precise analysis, and detection of electrical trees in high-voltage experiments. Integrating image filtering techniques during the preprocessing stage can further enhance these results by eliminating unwanted noise from the original treeing image. Additionally, introducing an advanced edge tracking segmentation technique as a complement to the existing method could enhance the sensitivity rate and further improve the overall segmentation process. The successful application of such techniques can aid researchers in understanding the behaviour and characteristics of electrical trees in insulating materials, contributing to advancements in electrical insulation technology and ensuring reliable power transmission and distribution systems.

**Acknowledgement**
The authors would like to thank the Ministry of Higher Education Malaysia for financially supported under the Fundamental Research Grant Scheme (FRGS/1/2020/TK0/UNIMAP/ 02/17).

**References**

[1] Zhang, Yuanyuan, Shengtao Li, Jian Gao, Shihang Wang, Kangning Wu, and Jianying Li. "Ageing assessment of XLPE cable insulation by residual antioxidant content." *IEEE Transactions on Dielectrics and Electrical Insulation* 27, no. 6 (2020): 1795-1802. https://doi.org/10.1109/TDEI.2020.008587

[2] Su, Jingang, Boxue Du, Jin Li, and Zhonglei Li. "Electrical tree degradation in high-voltage cable insulation: progress and challenges." *High Voltage* 5, no. 4 (2020): 353-364. https://doi.org/10.1049/hve.2020.0009

[3] Hamadi, S. H. K., M. Isa, L. M. Ishak, M. N. K. H. Rohani, C. C. Yii, B. Ismailf, and M. Shafiq. "Modelling of partial discharge signal and noise interference using labview." In *2017 IEEE 15th Student Conference on Research and Development (SCOReD)*, pp. 451-455. IEEE, 2017. https://doi.org/10.1109/SCORED.2017.8305441

[4] Rohani, M. N. K. H., M. Isa, M. Syahril, C. C. Yii, A. S. Rosmi, and B. Ismail. "Sigma-delta ADC topology implementation based on partial discharge detection using rogowski coil sensor." In *Journal of Physics: Conference Series*, vol. 1019, no. 1, p. 012031. IOP Publishing, 2018. https://doi.org/10.1088/1742-6596/1019/1/012031

[5] Hamadi, S. H. K., M. Isa, L. M. Ishak, M. N. K. H. Rohani, C. C. Yii, B. Ismail, and M. Shafiq. "Evaluation of denoising performance indices for noisy partial discharge signal based on DWT technique." In *2017 IEEE 15th Student Conference on Research and Development (SCOReD)*, pp. 392-397. IEEE, 2017. https://doi.org/10.1109/SCORED.2017.8305358

[6] Abdullah, A. Z., M. N. K. H. Rohani, M. Isa, H. Hamid, S. N. M. Arshad, and M. Othman. "Real on-site partial discharge measurement technique in medium voltage power cable." In *2018 IEEE 7th International Conference on Power and Energy (PECon)*, pp. 405-408. IEEE, 2018. https://doi.org/10.1109/PECON.2018.8684134

[7] Isa, MA Mohd, M. N. K. H. Rohani, A. S. Rosmi, M. Isa, N. Rosle, W. A. Mustafa, I. N. Daniel, and M. A. Roslan. "Investigation on partial discharge activities in cross-linked polyethene power cable using finite element analysis." In *Journal of Physics: Conference Series*, vol. 1432, no. 1, p. 012024. IOP Publishing, 2020. https://doi.org/10.1088/1742-6596/1432/1/012024

[8] Su, Yu, Ying Liu, and Lisheng Zhong. "Evaluation of voltage endurance characteristics for new and aged XLPE cable insulation by electrical treeing test." *IEEE Transactions on Dielectrics and Electrical Insulation* 26, no. 1 (2019): 72-80. https://doi.org/10.1109/TDEI.2018.007442

[9] Lv, Zepeng, Simon M. Rowland, Siyuan Chen, Hualong Zheng, and Ibrahim Iddrissu. "Evolution of partial discharges during early tree propagation in epoxy resin." *IEEE Transactions on Dielectrics and Electrical Insulation* 24, no. 5 (2017): 2995-3003. https://doi.org/10.1109/TDEI.2017.006731

[10] Rowland, Simon M., Roger Schurch, Michalis Pattouras, and Qi Li. "Application of FEA to image-based models of electrical trees with uniform conductivity." *IEEE Transactions on Dielectrics and Electrical Insulation* 22, no. 3 (2015): 1537-1546. https://doi.org/10.1109/TDEI.2015.7116349

[11] Isa, M. A. M., M. N. K. H. Rohani, B. Ismail, A. S. Rosmi, M. Isa, W. A. Mustafa, M. Kamarol, N. S. Mansor, and N. S. M. Nazar. "Review of Edge-based Image Segmentation on Electrical Tree Classification in Cross-linked Polyethylene (XLPE) Insulation." In *Journal of Physics: Conference Series*, vol. 1878, no. 1, p. 012012. IOP Publishing, 2021. https://doi.org/10.1088/1742-6596/1878/1/012012

[12] Tan, Siu Fong, and Nor Ashidi Mat Isa. "Exposure based multi-histogram equalization contrast enhancement for non-uniform illumination images." *Ieee Access* 7 (2019): 70842-70861. https://doi.org/10.1109/ACCESS.2019.2918557

[13] Wang, Yanfang, Qian Huang, and Jing Hu. "Adaptive enhancement for non-uniform illumination images via pixel-wise histogram modification and color reconstruction." In *2018 IEEE 3rd International Conference on Signal and Image Processing (ICSIP)*, pp. 220-224. IEEE, 2018. https://doi.org/10.1109/SIPROCESS.2018.8600429

[14] Abdulah, Cik Siti Khadijah, Mohamad Nur Khairul Hafizi Rohani, Baharuddin Ismail, Mohd Annuar Mohd Isa, Afifah Shuhada Rosmi, Wan Azani Wan Mustafa, Ahmad Zaidi Abdullah, Wan Nor Munirah Ariffin, and Mohamad Kamarol Mohd Jamil. "Review Study of Image De-Noising on Digital Image Processing and Applications." *Journal of Advanced Research in Applied Sciences and Engineering Technology* 30, no. 1 (2023): 331-343. https://doi.org/10.37934/araset.30.1.331343

[15] Dissado, Len A., and John C. Fothergill. *Electrical degradation and breakdown in polymers*. Vol. 9. Iet, 1992. https://doi.org/10.1049/PBED009E

[16] Ha, T., J. G. Su, T. T. Ma, F. Y. Wang, Y. Q. Xing, and Y. Gao. "Partial Discharge Characteristics During Treeing Process in Silicone Rubber at 20 and-100 degrees C." *IEEE TRANSACTIONS ON APPLIED SUPERCONDUCTIVITY* 29, no. 2 (2019). https://doi.org/10.1109/TASC.2018.2890516

[17] Huang, Sijay, Timothy B. Boykin, Ravi S. Gorur, and Biswajit Ray. "Electrical tree formation in polymer-filler composites." *IEEE Transactions on Dielectrics and Electrical Insulation* 26, no. 6 (2019): 1853-1858. https://doi.org/10.1109/TDEI.2019.008186

[18] Ohta, Tsukasa, and Kazuo Iida. "Dehydration reaction effect of metal hydroxide on AC voltage lifetime of epoxy composites." *IEEE Transactions on Dielectrics and Electrical Insulation* 23, no. 4 (2016): 2294-2302. https://doi.org/10.1109/TDEI.2016.7556506

[19] Kim, Thae Song, and Su Hyon Kim. "An improved contrast enhancement for dark images with non-uniform illumination based on edge preservation." *Multimedia Systems* 29, no. 3 (2023): 1117-1130. https://doi.org/10.1007/s00530-022-01042-1

[20] Benjamin Kommey, John Kwame Dunyo, Eric Tutu Tchao, and Andrew Selasi Agbemenu. “A Comparative Study of Common Edge Detection Operators in Digital Image Processing,” *Journal of Research in Engineering and Applied Sciences*, vol. 6, no. 4, (2021): 147–152. https://doi.org/10.46565/jreas.2021.v06i04.001